

Characterization of Rice Hull Ash

D. S. Chaudhary, M. C. Jollands

Rheology and Materials Processing Centre, Department of Chemical Engineering, School of Civil and Chemical Engineering, Royal Melbourne Institute of Technology, Melbourne, Australia 3000

Received 11 June 2003; accepted 12 November 2003

DOI 10.1002/app.20217

Published online in Wiley InterScience (www.interscience.wiley.com).

ABSTRACT: Rice hulls, a byproduct of the rice industry, contain 60–90% silica and are unique within nature. The annual worldwide output of rice-hull-derived silica is more than 3.2 million tons, which poses environmental concerns because of disposal issues. Burning rice hulls, as a preparative step for energy production, is a useful solution to the growing environmental concern, a desirable outcome would be the economic use of the resulting silica-rich hull ash. The economical usefulness of this silica ash in the filler market has been undermined by its limited dispersion abilities and poor interaction capability with polymers. In this study, some of the reasons for the poor performance of silica ash as a reinforcing filler in various polymeric composites were linked to its inherent characteristics: factors such as its impurity, irregular topography, porosity, and chemical and thermodynamic nature arising from its surface polarity that negatively influence the filler–matrix interactions. The silica ash obtained from a novel combustion process had about 6% (w/w) impurity, of which around 3% was volatile. We also

propose that the silanation efficiency of silica ash is lower compared to other commercial silicas because of its porosity, which could hide a fraction of the silane used. Also, processing changed the particle size distribution, and this could have affected the agglomerating tendencies and seriously marked the reinforcing capabilities of the silica ash. The estimation of the surface silanol groups of the rice hull ash by thermogravimetric studies indicated that the surface silanol density was about 16/nm². On a comparative scale, this value is comparable to the silanol density on precipitated silica, but a thermodynamic study of silica ash surface revealed a high surface free energy that contributed to its high aggregation tendencies and poor distribution and dispersion abilities. © 2004 Wiley Periodicals, Inc. *J Appl Polym Sci* 93: 1–8, 2004

Key words: fillers; structure-property relations; thermogravimetric analysis

INTRODUCTION

Rice hulls have an unusually high silica content.^{1,2} Yoshida et al. found that silica is distributed mainly in the outer layer of the hull in the prevalent form of silica gel.³ The nature of silica is mainly amorphous and has been termed *opaline silica*.⁴ With rice production only second to wheat production worldwide, the process produces an abundance of this scaly residue that corresponds to around 3.2 million tons of silica.⁵ Burning—and thus producing energy—is a cheap method of extracting the silica from the hulls for possible commercial use, but this has the associated problems of uncontrolled particle size and variable impurity levels (mainly in the form of intimately mixed carbon).

Because of growing environmental concern and the need to conserve energy and resources, efforts have been made to burn the husks under controlled conditions and to utilize the resultant ash in a variety of end

products.^{6–8} There have been some attempts to include this silica ash in a variety of polymers as fillers, in lieu of precipitated or fumed silica, to obtain composites with the goal of expanding the present filler market, but most investigations have indicated poor filler–matrix interactions and only moderate improvement in composite properties.^{9–13} This article presents a detailed investigation on the structure–property relations for silica ash in terms of physicochemical and thermodynamic characterizations aimed at improving the understanding of the behavior of silica ash in polymeric systems. Further, this study highlighted the importance of particle characteristics as a twofold effect on composite mechanical properties and emphasized that performance was strongly linked to the intrinsic properties of silica ash. First, from a physical point of view, characteristics such as high impurities, particle shape, and porosity affected the agglomeration tendencies and particle–matrix interactions. Second, from a thermodynamic point of view, the topography and surface active sites affected the efficiency of surface modification. Combinations of such characteristics in turn limited its reinforcing character. One report identified the importance of the structure–function relation for various commercial silicas and stated that the best reinforcing character results from a high surface area, a low-median agglomerate particle size,

Correspondence to: D. S. Chaudhary.

Contract grant sponsor: Ricegrowers Cooperative, Ltd.

Contract grant sponsor: Rheology and Materials Processing Centre, Royal Melbourne Institute of Technology.

and a low adsorbed moisture.¹⁴ Silica ash, however, is a byproduct of a natural compound, and such characterization studies on silica ash have not been undertaken, which leaves scope for further investigation to understand the reasons for its inferior behavior and to study the modifications necessary to improve the mechanical properties of silica ash composites.

EXPERIMENTAL

Filler preparation

Silica ash was obtained from Biocon Industries (Griffith, Australia). It was washed in an acidic aqueous solution (pH \approx 4.5) and was then with distilled water to remove the metal impurities and surface carbon. Then, it was dried at 60°C overnight. Density measurements carried out with a water pycnometer, and the particle density was found to be 1.83 g/cm³ with a bulk density of 0.22–0.25 g/cm³.

Composite preparation and effect of processing

A Haake Rheocord batch mixer. Rheomex model with Haake Rheocord software, Haake Instruments, Germany; capacity = 66cm³) was used to prepare all of the composites with 20% (w/w) filler content. To determine the processing effects on the particle size, the composites were mixed for a given period and were then removed from the mixer. These samples were subjected to a temperature of 500°C for 2 h to burn off the polymer and to obtain the silica ash. For particle size analysis, a small sample of silica ash was loaded in an automated Malvern Sizer (MastersizerX version 1.1, Malvern Instruments). Sodium tetrphosphate (0.5 g) was added in deionized water as a dispersing agent, and subsequently, a sufficient quantity of the sample was added to produce statistically good data (as indicated by the automatic sampler). The mixture was sonicated during the analysis to prevent agglomeration.

Surface area measurements

Surface area measurements were carried out in a Micrometrics ASAP 2000 with ASAP 2000 software version 3.03 with the BET isotherm method. The silica ash was pretreated in an oven at 200°C at atmospheric pressure for 2 h to remove volatile compounds before the surface area analysis. We carried out the surface area analysis by evacuating the sample chamber at very low pressures and then allowing nitrogen into the chamber. A set of three samples were analyzed the silica ash had a surface area of about 29 m²/g (standard deviation = 0.54) with a cumulative pore surface area of about 12 m²/g and an average pore diameter of about 71 Å.

Thermogravimetric (TGA) measurements

TG studies were carried out to estimate the hydroxyl group density on the silica ash surface and the sample purity with a PerkinElmer TG analyzer (TGA 7/TAC7DX with Pyris software version 3.81). Microgram samples (\sim 5 μ g) of silica ash were carefully loaded in the pan and subjected to a constant heating rate from room temperature to 800°C in an inert atmosphere, and the weight loss against temperature was recorded. Automated baseline correction was used, and the fractional weight loss between two given temperature points was found graphically. If the sample weight loss between 350 and 800°C in an inert atmosphere corresponded to the amount of condensation water lost from silanol groups, the amount of water lost could have been directly related to the density of the silanol groups.¹⁵ Because the condensation of two silanol groups gives one water molecule, if m grams of condensation water is lost, the number of silanol groups is $n = 2Nm/18$, where N is Avogadro's number. Where the BET area is x and the sample weight is w , the number of silanol groups (nm²) is $(2b * 1000)/3xw$, where $b = m/100 = \% \text{ Weight loss}$.

Thermodynamic studies

The surface energetic of the silica ash was determined by with a gas chromatograph (Shimadzu 8A, Japan) with a flame ionizing detector at infinite dilution. A 304.8 mm long nickel column with an ID of 2.11 mm was packed with the standard technique with silica ash particles. Before it was packed, the silica ash was dried overnight at 110°C. The packed column was sealed with glass wool and conditioned overnight at 210°C. Injectordetector temperatures were maintained at 220°C, and measurements were carried out at 60, 80, and 100°C with helium as the carrier gas at a flow rate of 20 mL/min. Approximately 0.5 μ L of probe was injected, and retention times were determined graphically. With De-Boer's state of reference, the required surface energy parameters were estimated according to a procedure described elsewhere.^{16,17} Table I lists the various probes used to estimate the surface energetics of the silica ash.

RESULTS AND DISCUSSION

Particle size determination

Most investigations into the effect of filler particle size on polymeric composite properties have enumerated that particle size is inversely related to the reinforcing character and that an increase in surface area (as a consequence of reduced particle size) increases the composite mechanical properties.^{18,19} However, it is well known that small particles with higher specific surface areas tend to agglomerate because of increased

TABLE I
Various Polar and Nonpolar Probes Used for the Determination of the Surface Energetics of the Silica Ash

Probe	Molecular weight	a (\AA^2)
Pentane	60	45.5
Hexane	72	51.5
Heptane	84	57
Octane	96	63
Acetone	58	42.5
Chloroform	64	44
THF	72	45

a = theoretical molecular weight reported in ref. 16.

filler–filler interactions. In reality, a good homogeneous filler distribution rarely occurs, and the reduction of particle size and its aggregation tendencies need to be balanced.

Figure 1 shows the result of the particle size analysis from the Malvern Sizer software for the silica ash. It indicates that the distribution was centered near 50 μm . The occurrence of a broad shoulder (between 8 and 25 μm) indicated that a significant number of particles were in this range. Blume suggested that larger particles in the peak region might be secondary agglomerates that can break down to give smaller particles and thus increase the volume fraction of smaller particles in the final composite, producing a better reinforcing character.²⁰ This could result in a broad bipolar distribution. During processing, however, smaller particles in the distribution may also aggregate to give a different sized distribution in the composite, reduce filler distribution, and reduce its reinforcing character. Table II shows the results for the silica ash particle size distribution and the effect of processing on the average particle size. The large standard deviation associated with the median size and the shape of Figure 1 indicated that the distribution was broad rather than bipolar.

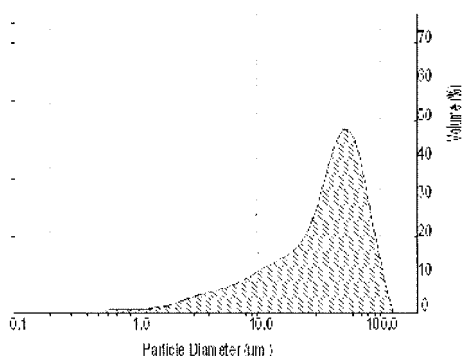


Figure 1 Particle size distribution for the silica ash (median size = 47 μm).

TABLE II
Size Distribution (μm) of Silica Ash as Affected by Processing (Mixing) Times

Volume fraction (%)	Before processing	After processing		
		7 min	10 min	15 min
10	14	5	4	5
20	26	10	10	10
50	50	34	34	33
Mean	47 (24)	34 (12)	33 (12)	33 (11)

The values in bracket indicate the standard deviation.

Table II shows the effect of processing on the particle size. There was a reduction in particle size during processing, and this generated a broader size distribution. This, along with increased agglomeration tendencies and the more irregular shape, would reduce the filler packing capacity, the dispersion, and the reinforcing character of silica ash in polymeric composites.

Controlling the particle size during the burning process is not economically viable. The data obtained for silica ash from Industries,²¹ who produce commercial silica ash in an economically viable way, showed that the particle size was controlled only to a moderate extent (as seen by the broad distribution in Fig. 1), and experimental investigations regarding the optimum particle size of silica ash for reinforcement have yet to be reported.

Impurity in silica ash

Impurities in silica ash occur as surface carbon or as carbon trapped in the silica ash structure along with some volatile matter associated with silica ash.²² Investigations have found that temperature plays a significant role in the level of carbon associated with the silica in silica ash by influencing a cocoon structure of silica that at high temperatures, traps the carbon, and thus, the burning of the hulls inherently includes carbon as an impurity.^{22,23}

Figure 2 is a thermogram showing the weight loss curves of two samples of silica ash, one in an oxygenated (air) atmosphere and the other one in an inert (N_2) atmosphere, against temperature in a TG experiment carried out at a constant heating rate of 10°C/min. In a N_2 atmosphere, the carbon was not oxidized, and the total weight loss represented the net volatile matter, and the total amount of carbon in the silica ash sample could be found by the subtraction of the weight loss in N_2 from the weight loss in air.

As shown in Figure 2, the weight loss at low temperatures indicated the loss of adsorbed moisture and other volatile compounds, and as expected, the slopes of the two curves were similar. As temperature increased, there was a progressive loss in matter in both

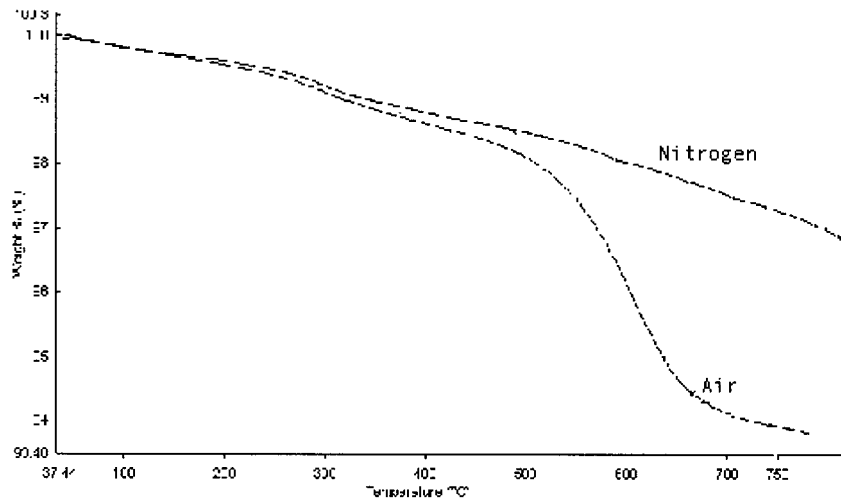


Figure 2 Typical thermogram of silica ash comparing the weight loss values in nitrogen and oxygen atmospheres. Silica ash was evacuated at 100°C.

samples; however, in air, carbon was converted to CO_2 at around 500°C, as reflected by the change in the slope of the corresponding curve. In N_2 , carbon was not lost, but the relatively slow weight loss step in the broad region between 300 and 800°C indicated silanol group condensation and maybe some elemental decomposition. The analysis showed that the percentage purity of the silica ash sample was about 94 wt % silica, and the carbon content was about 3%. Experiments conducted with other heating rates (5, 12, and 20°C/min) showed similar results.

Estimation of silanol groups

Silanol ($-\text{OH}$) groups are reactive groups known to dominate the filler–matrix adhesion,^{24,25} and in an epoxy matrix, they increase the polymer hardness by crosslinking polymeric chains.^{26–28} However, these groups take up moisture and/or interact among themselves to neutralize one another and cause filler agglomeration. The surface silanol group density for the silica ash was calculated with TG techniques. Figure 3 is a thermogram of silica ash in an inert (N_2) atmosphere. The weight loss occurred through two steps, first through the removal of physically adsorbed water (and some small molecules trapped in the pore structure), occurring up to about 250°C, and second through the removal of chemical water by the condensation of two silanol groups, occurring between 350 and 800°C. It can be seen (from the difference in slopes) that the first reaction (100–250°C) was quite rapid and short compared to the second step (350–800°C), which occurred over a broader temperature range. Above 850°C, elemental decomposition and morphological changes occur in the silica ash structure, as described elsewhere.²⁹ On the basis of the BET

surface area and an average second step weight loss of 0.72 wt % for a number of silica ash samples in N_2 , the average number of silanol groups was estimated to be about 16/nm². In comparison, the reported temperature range for precipitated silica was 270–700°C with about 13 silanol groups/nm²,²⁹ whereas fumed silicas contain about 4.5 primarily isolated silanol groups/nm².³⁰ A previous investigation suggested that the density of silanol groups is not sufficient enough for good particle–matrix interaction; however, we believe that the high temperature treatment (>1000°C) used in that study might have rendered the surface hydrophobic.¹⁵ This suggests that surface quality of silica ash depends largely on the production temperature.

The higher number of silanol groups, which are known to react with surface-modifying agents, are, the higher the compatibility of the treated silica is with polymers, especially those having reactive groups toward silanol, such as natural rubber with the epoxy groups. However, with fillers added on a weight or volume basis, a simple analysis of silanol groups per

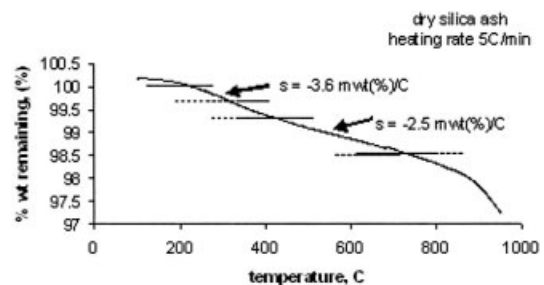


Figure 3 Thermogram showing the weight loss curve at a constant heating rate for a silica ash sample in an inert atmosphere of nitrogen. The slope (s) is given in units $\text{mwt}(\%)/^\circ\text{C}$, that is, $10^{-3} \text{ wt } \% (\%)/^\circ\text{C}$.

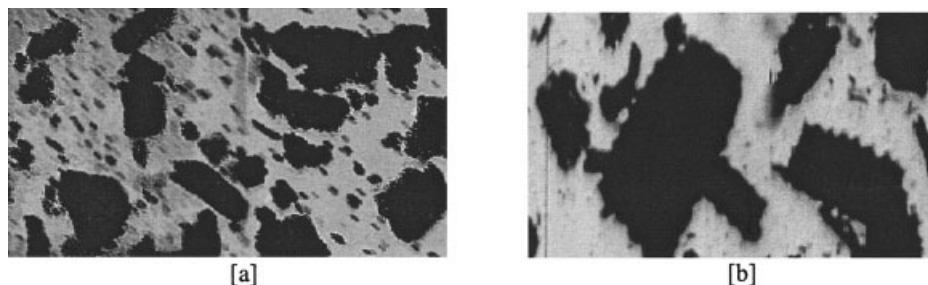


Figure 4 Micrograph of silica ash particles (a) dispersed in a solution of sodium tetraborate and (b) showing the irregular topography of the particle.

gram of filler indicated that silica ash had an inferior silanol group density per gram. When we compared commercial precipitated silica or fumed silica (both having surface areas $> 100 \text{ m}^2/\text{g}$ but silanol densities of ~ 9 and 4.5 groups/ nm^2 , respectively) with silica ash (surface area $\approx 29 \text{ m}^2/\text{g}$ and silanol density ≈ 16 groups/ nm^2), the silanol group per gram of precipitated silica ($\sim 900 \times 10^{18}$) and fumed silica ($\sim 450 \times 10^{18}$) was higher than that of silica ash ($\sim 320 \times 10^{18}$). Both precipitated silica and silica ash were amorphous and irregular, but the surface treatment was more effective for precipitated silica because of its higher silanol group density per gram. Fumed silica, with a flat and plane structure, had an efficient surface treatment. Therefore, compounded with higher impurity level and porosity, both factors, surface irregularity and a lower silanol group density per gram, acted against the reinforcing character of silica ash, as shown by various experimental investigations.^{31–34}

Particle surface area and porosity

Nitrogen BET surface area measurements were carried out on an evacuated sample of silica ash (the sample was conditioned at 100°C overnight). The silica ash had a specific surface area of about $29 \text{ m}^2/\text{g}$ with a cumulative pore volume of about $0.03 \text{ cm}^3/\text{g}$ and a cumulative pore area of about $12.5 \text{ m}^2/\text{g}$. The average pore diameter was about 71 \AA .

Porous particles such as silica ash could hide moisture or other smaller molecules (e.g., N_2 , CO_2) in their pore structures. These could change final composite properties unfavorably, as residual molecules can cause voids or debonding in composites.³⁵ More important, during the silane treatment of silica ash particles, a fraction of the silane molecules used for surface treatment could also be lost in the pore structure.³⁶ It is possible that silane molecules, with an average molecular cross-sectional area of 50 \AA^2 ,³⁷ would traverse into the pore structure of silica ash (average pore diameter $\approx 71 \text{ \AA}$), whereas the steric hindrances of long polymeric chains would limit their access into the pores, and consequently, the overall silanation efficiency would be reduced.

Particle shape

It is known that for particulate fillers, irregularity reduces the silanation and the filler packing efficiency,^{19,24} and surface topography influences the filler reinforcing character.²⁶ Figure 4 shows a micrograph of a silica ash sample and shows that there was some degree of particle irregularity, which probably added to its poor performance.

Figure 4(b) shows that silica ash retained its serrated structure despite the burning process, and its topography was irregular. As mentioned earlier, such irregularity could affect the silanation efficiency, a situation schematically shown in Figure 5. Figure 5 shows that it was easier for smaller water molecules to access these sites, which may have compromised the improvement in filler–matrix adhesion and permanently deteriorated the composite mechanical properties.³⁸ Hence, these silica ash particle characteristics are not optimal for its reinforcing character, and a more uniform particle size and shape (and possibly a lower average size to minimize structural breakdown) is required.

Surface energy measurements

Recent investigations have highlighted the shifting focus onto the study surface energetics to understand

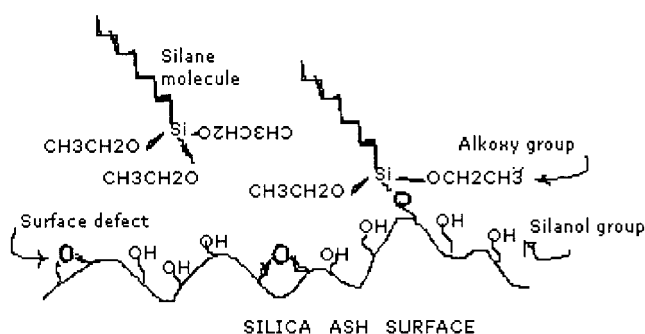


Figure 5 Schematic representation of the silica ash surface showing the limited accessibility of silane molecules for the capping of silanol groups.

TABLE III
Surface Energy Components of Commercial Carbon Black and Precipitated Silica⁴⁰

Filler	γ^d (mJ/m ²)	γ^{sp} (mJ/m ²)
Carbon black N110	270.4	1.63
Precipitated silica	22.9	3.58

γ^d and γ^{sp} represent the dispersive and specific interaction components, respectively, of the surface energy.

the aggregation and surface modification of filler particles and have indicated the significance of thermodynamic events underlying various processes.^{39,40} As an example for understanding performance on the basis of surface energetics, the difference in dispersive and specific interaction components of the surface energy of carbon black and precipitated silica⁴⁰ is shown in Table 3. It shows that the higher agglomeration tendencies of commercial precipitated silica could be expressed as a function of its surface energy, specifically the dispersive component, and highlights the superiority of carbon black as a reinforcing filler.

For silica ash, IGC studies were used to determine its surface energy components. The retention times of standard solutes, affected by their interactions with the stationary phase, were estimated and converted into the components of surface energy with standard methods.^{41–43} Table IV shows the time retention (T_r) data and the free energy of adsorption (ΔG) values measured at three different temperatures.

For homologous *n*-alkanes (apolar probes) interacting with silica, the free energy of adsorption (ΔG^{alkane}) varied linearly with the corresponding carbon number, as shown in Figure 6. This was due to the absence of any specific interactions.

Figure 6 also shows the temperature dependence of ΔG^{alkane} , which decreased with increasing temperature as expected. This was due to the increase in the degree of freedom of the probe molecules, which made adsorption difficult.⁴⁰ γ^d was obtained from the derivative of ΔG per mole of methylene groups (CH_2).⁴¹

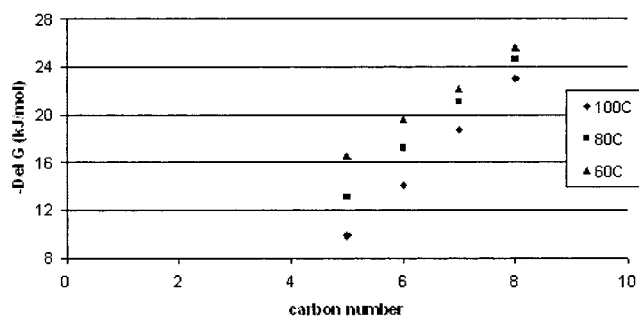


Figure 6 Variation in surface energy of silica ash particles against the alkane homologous series ($\text{C}_5\text{--}\text{C}_8$) at different temperatures.

The interaction of polar probes, however, involved both dispersive and specific interactions, and in practice, when ΔG , corresponding to alkane and polar probes (ΔG^{polar}) was plotted against the molecular cross-sectional area (a), The values of ΔG^{polar} were above the reference line given by the ΔG^{alkane} values. For any polar probe, γ^{sp} is then taken as the difference between ΔG^{polar} and ΔG^{alkane} , where the corresponding alkane has similar physicochemical property to the polar probe.⁴³ The nature of the probe dictates its separation from the *n*-alkane reference line. This is shown in Figure 7, where various probes were above the reference line according to their capability to interact with the silica ash surface.

Figure 7 also suggests the nature of the silica ash surface. The *n*-alkane reference line represents the zero tendency to accept or donate electrons. The basic tetrahydrofuran (THF) was situated further from the alkane line than the acidic chloroform (CHCl_3), as THF interacted more strongly compared to CHCl_3 , indicating that the silica ash surface was acidic in nature. γ^d and γ^{sp} of silica ash for various polar probes are reported in Table V.

Interestingly, Figure 8 shows that the decrease in γ^d was not linear, and the temperature dependence of γ^d could be described as

TABLE IV
Retention Data of Various Probes and Surface Energy of Silica Ash as Measured at Three Different Temperatures

Probe	100°C		80°C		60°C	
	T_r (min)	$-\Delta G$ (kJ/mol)	T_r (min)	$-\Delta G$ (kJ/mol)	T_r (min)	$-\Delta G$ (kJ/mol)
C5	0.200	12.646	0.221	12.350	0.271	12.246
C6	0.488	16.030	0.652	16.282	0.898	16.414
C7	1.425	19.672	2.480	20.447	4.052	20.823
C8	5.228	23.799	11.240	24.948	20.457	25.359
THF	1.650	20.091	3.052	21.071	6.252	22.047
CHCl_3	0.488	16.030	0.550	15.719	0.580	15.024
Acetone	1.157	18.941	1.328	18.540	1.775	18.453

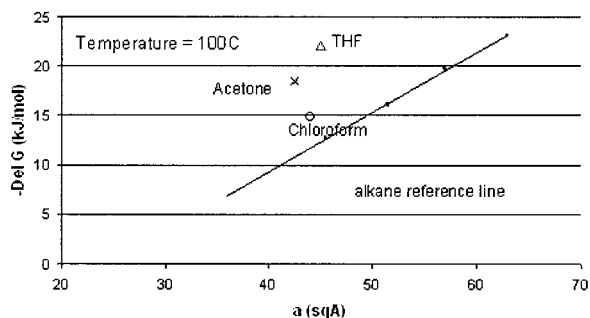


Figure 7 Surface energy of various polar probes and their separation from the *n*-alkane reference line for silica ash at 100°C.

$$\frac{d\gamma^d}{dT} = -0.0159T + 1.702 + c[\text{mJ}/(\text{°C m}^2)]$$

where T is the temperature and c is a constant.

The behaviour of γ^{sp} was similar to its dispersive counterpart. The higher γ^{sp} of silica ash with THF or acetone as against CHCl_3 probe was a reflection of the higher surface polarity that allowed silica ash to interact strongly due to its acidic silanol groups. Further, changes in temperature had a significant effect on γ^{sp} for basic THF compared to amphoteric acetone. This was expected because with a decrease in temperature and freedom, it was easier for the species to interact, and because it was basic in character, the increase in the interaction parameter was highest for THF.

The results showed a poor silanol group density per gram and indicated a relation between the poor dispersion characteristics and low γ^d/γ^{sp} ratio of silica ash. Such characteristics of silica ash along with its irregular shape and porosity could also explain the inferiority in performance compared to other commercial silica fillers with similar surface free energies^{44,45} and suggest that

CONCLUSIONS

Past investigations have clearly indicated that there are certain issues with silica ash that must be resolved for it to be used as a reinforcing agent in polymeric composites. A systematic method to approaching the observed behavior of silica ash is the characterization

TABLE V
 γ^d γ^{sp} at Various Temperatures

Temperature (°C)	γ^d (mJ/m ²)	γ^{sp} (mJ/m ²)		
		THF	CHCl_3	Acetone
100	75.39	28.95	10.16	32.05
80	98.63	33.842	13.33	32.83
60	106.23	37.95	14.65	33.44

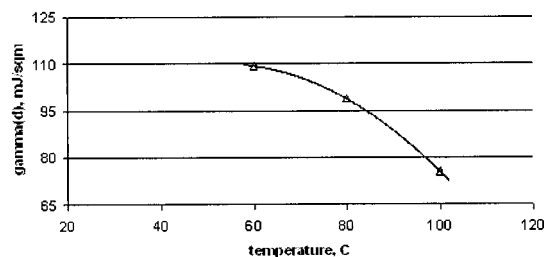


Figure 8 Influence of temperature on γ^d of silica ash.

of the materials as detailed in this investigation. Issues such as filler aggregation and poor filler–matrix adhesion, widely mentioned in literature, can now be understood in terms of the combined effect of a low surface area and a high surface polarity (low ratio of γ^d to γ^{sp}) of silica ash. The impurity level and particle porosity could explain its limited capability to undergo silanation.

It is accepted that the impurity level is silica ash is related to its production conditions, which differ in different parts of the world. However, most investigations have indicated the use of high-purity silica ash (~5%), which is similar to the material investigated in this study. Further, because the nature of silica ash remains similar due to identical production methods, analysis of the behavior of silica ash on the basis of its characteristics would retain its generality. We suggest here that the improvement in the mechanical properties of silanated silica ash–polymer composite is compromised by the presence of surface impurities and the structural breakdown of silica ash during processing that generates irregular particles with poor reinforcing characteristics.

In this investigation, analytical methods, such as TG analysis and IGC, were successfully used to estimate the physicochemical properties of silica ash. Interestingly, as revealed by TG analysis, the silica ash used in this study possessed adequate surface silanol groups to undergo efficient silanation and to therefore provide better interaction with a polymer. Further investigations are required to understand silanation of silica ash from a thermodynamic point of view. Also, there is strong evidence that the poor filler–matrix adhesion can be improved by an increasing the surface area (by reducing the particle size) for increased interaction and subsequent silanation.

The authors acknowledge the contribution of Dr. Cser in the form of valuable discussion and the support of Mr. Chryss for forwarding comments on the particle size analysis.

References

- Lanning, F. C. *J Agric Food Chem* 1963, 11, 435.
- Houston, D. F. *Rice Chemistry And Technology*; American Association of Cereal Chemists: St. Paul, MN, 1972; p 301.

3. Yoshida, S.; Ohnishi, Y.; Kitagishi, K. *Soil Sci Plant Nutr* 1962, 8, 29.
4. Beagle, E. C. *FOA Agric Services Bull* 1978, 31, 8.
5. Natarajan, E.; Nordin, A.; Rao, A. N. *Biomass Energy* 1998, 14, 533.
6. Jin, Z. C.; Jia, L. Y.; Jia, X. C. *Cellul Chem Technol* 1992, 26, 345.
7. Barkakati, P.; Bordoloi, D.; Borthakua, P. C. *Cem Concr Res* 1994, 24, 613.
8. Krishnarao, R. V. *J Eur Ceram Soc* 1993, 12, 395.
9. Fuad, M. Y. A.; Jamaludin, M. *Int J Polym Mater* 1993, 19, 75.
10. Ishak, Z. A. M.; Bakar, A. A.; *Eur Polym J* 1995, 31, 259.
11. Fuad, M. Y. A.; Ismail, Z.; Ishak, Z. A. M.; Omar, A. K. M. *J Elast Plast* 1994, 26, 252.
12. Ismail, H.; Nasaruddin, M. N.; Rozman, H. D. *Eur Polym J* 1999, 35, 1429.
13. Ismail, H.; Nasaruddin, M. N.; Ishiaku, U. S. *Polym Int* 1999, 18, 287.
14. Okel, T.; Waddell, W. *Am Chem Sec Rubber Div Conf Proc* 1994, 145(Spring), 44.
15. Hanna, S. B.; Farag, L. M. *Thermochim Acta* 1985, 87, 239.
16. Schultz, J.; Lavielle, L. In *Inverse Gas Chromatography: Characterisation of Polymers and Other Materials*; Llyod, D. R.; Ward, T. C.; Schreiber, H. P.; Pizana, C. C., Eds.; ACS Symposium Series; American Chemical Society: Washington, DC, 1988; Chapter 7.
17. Bovari, A. E.; Ward, T. C.; Koning, P. A.; Sheehy, D. P. In *Inverse Gas Chromatography: Characterisation of Polymers and Other Materials*; Llyod, D. R.; Ward, T. C.; Schreiber, H. P.; Pizana, C. C., Eds.; ACS Symposium Series; American Chemical Society: Washington, DC, 1988; Chapter 2.
18. Hepburn, C. *Plast Rubber Int* 1984, 9, 11.
19. Pukanszky, B.; Fekete, E. *Polym Polym Compos* 1998, 6, 313.
20. Blume, A. Presented at the 155th Meeting of the American Chemical Society Rubber Division, Chicago, IL, 1999; Paper 73.
21. Spiers, S. Biocon Industries, Australia. Private communication, 2001.
22. Krishnarao, R. V.; Subrahmanyam, J.; Jagadish, T. K. *J Eur Ceram Soc* 2001, 12, 99.
23. Chakraverty, A.; Mishra, P.; Banerjee, H. D. *J Mater Sci* 1988, 23, 21.
24. Nakamura, Y.; Okabe, S.; Iida, T. *Polym Polym Compos* 1999, 7, 177.
25. Fowkes, F. M. *Polym Sci Technol A* 1979, 12, 43.
26. Goritz, D.; Raab, H.; Frohlich, J.; Maier, P. *Rubber Chem Technol* 72, 929.
27. Nunes, R. C. R.; Fonseca, J. L. C.; Pereira, M. R. *Polym Test* 2000, 19, 93.
28. Manna, A. K.; Bhattacharyya, A. K.; De, P. P.; Tripathy, D. K.; De, S. K.; Peiffer, D. G. *Polym Int* 1998, 39, 7113.
29. Lin, J.; Siddiqui, J. A.; Ottenbrite, R. M. *Polym Adv Technol* 2001, 12, 285.
30. Markham, J. L.; Le Grange, J. D.; Kurkjian, C. R. *Annu Tech Con* 1993, 1148.
31. Ismail, H.; Khalil, H. P. S. A. *Polym Test* 2001, 20, 125.
32. Ishak, Z. A. M.; Yow, B. N.; Ng, B. L.; Khalil, H. P. S. A.; Rozman, H. D. *J Appl Polym Sci* 2001, 81, 742.
33. Fuad, M. Y. A.; Mansoor, M. S. *Polym Int* 1995, 38, 33.
34. Ismail, H.; Mega, L.; Khalil, H. P. S. A. *Polym Int* 2001, 50, 606.
35. Jelinek, L.; Dong, P.; Rojas-Pazos, C.; Taibi, H.; Kovats, E. S. *Langmuir*, 1992, 8, 2152.
36. Chaudhary, D. S.; Jollands, M. C.; Cser, F. *Silicon Chem*, to appear.
37. Plueddemann, E. P. *Silane Coupling Agents*; Plenum: New York, Press 1991; p 83.
38. Fuad, M. Y. A.; Ismail, Z.; Ishak, Z. A. M.; Omar, A. K. M. *Eur Polym J*, 1995, 31, 885.
39. Pukanszky, B.; Fekete, E. *Adv Polym Sci* 1999, 139, 109.
40. Wang, M. J.; Wolff, S. *Rubber Chem Technol* 1992, 65, 890.
41. Dorris, G. M.; Gray, D. G. *J Colloid Interface Sci* 1980, 77, 353.
42. Fowkes, F. M. *Ind Eng Chem* 1964, 56, 40.
43. Wang, M. J.; Wolff, S.; Donnet, J. B. *Rubber Chem Technol* 1991, 64, 559.
44. Voelkel, A.; Krystafkiewicz, A.; *Powder Technol* 1998, 95, 103.
45. Kimura, M.; Kataoka, S.; Tsutsumi, K. *Colloid Polym Sci* 2000, 278, 848.